MANCHESTER 1824
The University of Manchester
AkzoNobel

Simplified temperature distribution of 3 sides protected steel beam

MACE

Research Background

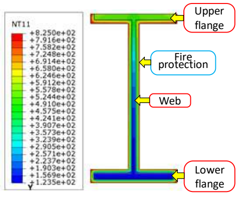

Typical temperature distribution of 3 sides protected steel beam

3 sides protected steel beam is a common practice in offshore facilities such as oil platform and refinery. Attachments such as pipes and gratings must be directly connected to the top surface of the upper flange of the steel section thereby preventing the upper flange from being attacted by fire. This causes a highly undesirable situation whereby the most critical part of the beam (compression flange) is almost unprotected and experiences high temperatures. On the other hand, the attachments may be able to provide sufficient lateral and torsional restraint to allow the 3-side protected steel beam to develop high bending resistance with little adverse effect from lateral torsional buckling. However, this industry inspired problem has received very limited systematic research investigation, leading to a variety of practices without solid supporting evidence.

Introducing k values to converge the realistic and theoretical heat flux

To minimise the gap of heat flux between realistic and numerical linear model in between each parts, two k values are introduced and derived by 98 transient heat transfer simulations considering section depth, flange and web thickness, thickness and conductivity of fire protection material and ratio of conductivity between flange and web protection.

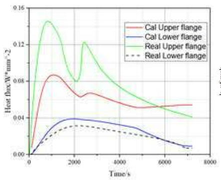

Comparison between Realistic and calculated Heat flux

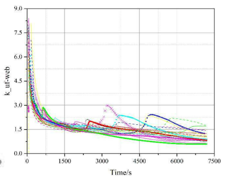

Typical k uf-web to time curve

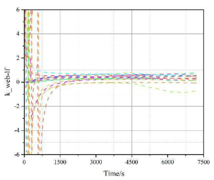

Typical k web-lf to time curve

Analysis of k value to depth

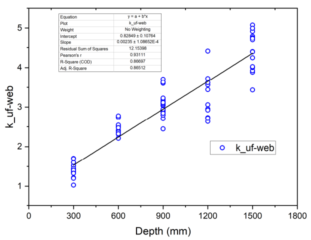

k uf-web to depth data points

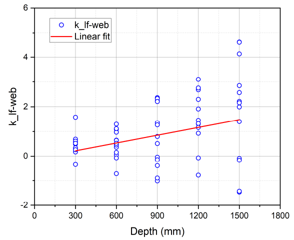

k lf-web to depth data points

Retrofitted lumped capacity model

Upper flange

$$\Delta\theta_{a,tu} = \frac{1}{C_a\rho_a}\frac{1}{V_t}\{A_{p,u,top}\{\underbrace{\alpha_c(\theta_t-\theta_{a,tu})}_{q_{convective}}+\underbrace{\varepsilon_m\varepsilon_f k_{stefan-boltzmann}[(\theta_t+273)^4-(\theta_{a,tu}+273)^4]}_{q_{radiative}}\}_{Q_{unprotected}} + \underbrace{A_{p,u,bottom+tip}\frac{1}{1+\omega/3}\frac{\lambda_p}{d_p}(\theta_t-\theta_{a,tu})}_{Q_{protected}} \quad (1)$$

$$\underbrace{-k_{uf-web}A_{junction}\frac{\lambda_a}{d_{web}}(\theta_{a,tu}-\theta_{a,tw})}_{Q_{top\ junction}}\}\Delta t \underbrace{-\frac{A_{p,u,bottom+tip}}{A_{p,u}}(e^{\frac{\omega}{10}}-1)\Delta\theta_t}_{Proportioned\ modification\ factor}$$

Web

$$\Delta\theta_{a,tw} = \frac{1}{C_a\rho_a}\frac{1}{V_t}[\underbrace{A_{p,w}\frac{1}{1+\omega/3}\frac{\lambda_p}{d_p}(\theta_t-\theta_{a,tw})}_{Q_{web}}+\underbrace{k_{uf-web}A_{uf-web}\frac{\lambda_a}{d_{tf-web}}(\theta_{a,tu}-\theta_{a,tw})}_{Q_{top\ junction}}-\underbrace{k_{web-bf}A_{web-bf}\frac{\lambda_a}{d_{web-bf}}(\theta_{a,tw}-\theta_{a,tb})}_{Q_{bottom\ junction}}]\Delta t \quad (2)$$

$$\underbrace{-(e^{\frac{\omega}{10}}-1)\Delta\theta_t}_{Modification\ factor}$$

Lower flange

$$\Delta\theta_{a,tb} = \frac{1}{C_a\rho_a}\frac{1}{V_t}[\underbrace{A_{p,b}\frac{1}{1+\omega/3}\frac{\lambda_p}{d_p}(\theta_t-\theta_{a,tb})}_{Q_{web}}+\underbrace{k_{web-bf}A_{web-bf}\frac{\lambda_a}{d_{web}}(\theta_{a,tw}-\theta_{a,tb})}_{Q_{bottom\ junction}}]\Delta t\underbrace{-(e^{\frac{\omega}{10}}-1)\Delta\theta_t}_{Modification\ factor} \quad (3)$$

For upper flange, the convective, radiative and conductive contribution from fire and the heat conduction between upper flange and web are considered through combination of EC3 equations and the Fourier's law. Besides, the reduction factor for conduction through insulation is modified in according to the reduced protected area.
For web and lower flange, the equation includes the heat conduction through insulation and conduction between web and flange.

Comparison between simulation and prediction

The predictions with k values below are compared with simulation results.

$$k_{uf-web} = 0.00235 * d + 0.825$$

$$k_{web-lf} = 0.00156 * d - 0.124$$

Comparison between prediction and cases with largest gaps are shown as :

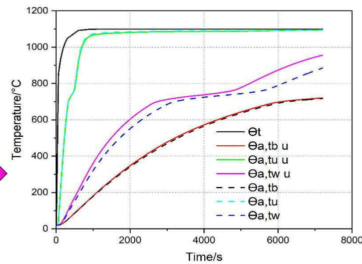

300x100x10x5con0.2it50 hydrocarbon fire

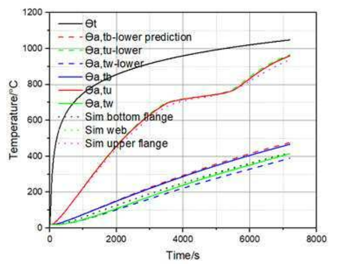

900x300x30x15 flange con0.2 web con0.02 it32

Extreme cases of between upper k value and prediction k value

Comparison between prediction and upper and lower k value curve show overall good convergence.

Incorporating web and flange thickness into prediction of k values

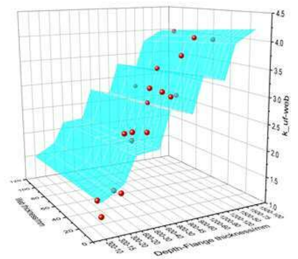

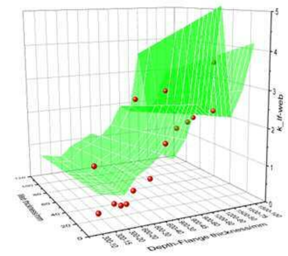

$$k_{uf-web} = \frac{(0.002*d+1.0622)*(-0.0005*t_w+1.0128)}{(-1.2E-5*(t_f/d-0.05)*d^2+0.024*(t_f/d-0.05)*d-10.674*(t_f/d-0.05)+1)}$$

$$k_{web-lf} = \frac{(0.0016*d+0.2402)*(-0.0032*t_w+1.1998)}{(3.6E-5*(t_f/d-0.05)*d^2-0.084*(t_f/d-0.05)*d+27.312*(t_f/d-0.05)+1.0353)}$$

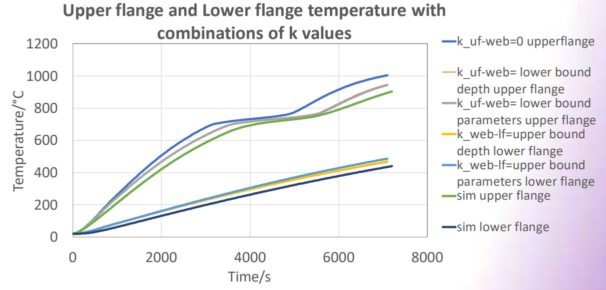

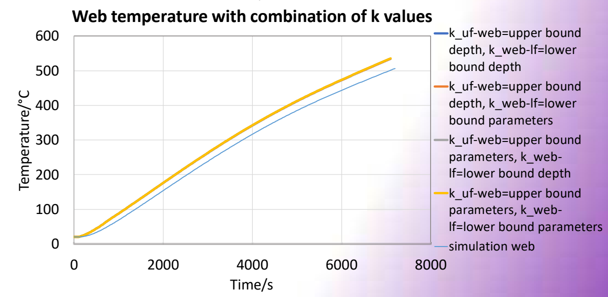

The lower limit of k_uf-web – depth, the upper limit of k_uf-web – depth and lower limit of k_lf-web – depth and the upper limit of k_lf-web – depth are chosen for calculating the temperature of Upper flange, web and lower flange. From comparison, the combination of k values achieves good balance between safety, simplicity and precision.

For more information, please contact
Supervisor: Yong Wang
Yang Li PhD student
E-mail：yang.li-45@postgrad.manchester.ac.uk

2022 MACE PGR Conference, 1st July 2022

Department of Mechanical, Aerospace and Civil Engineering